

form. Compound elastic scattering was accounted for by use of the theory of Hauser and Feshbach.<sup>20</sup>

The results of the calculations show fair agreement with the measured total and differential cross sections, especially for the case of Li<sup>7</sup>. The fits to the polarization measurements, on the other hand, were somewhat worse. Typical examples of the kind of agreement that was obtained are shown in Figs. 13 and 14. The solid curves on these figures show the calculations including compound elastic scattering. The dashed curves show only the shape-elastic predictions.

We have made preliminary attempts to improve the fits by studying the effect of varying some of the optical-model parameters. A variation of the parameters of the spin-orbit potential did not lead to improved agreement with the data when the values of the other parameters were kept fixed at those strengths predicted by the nonlocal model. Further variation of parameters from those predicted by the nonlocal model have led so far to only qualitative conclusions. For example, it appears that better agreement with the data might be obtained with somewhat smaller values for the strength of the imag-

<sup>20</sup> W. Hauser and H. Feshbach, Phys. Rev. 87, 366 (1952).

inary central potential. Recently, Perey and Saxon<sup>21</sup> have pointed out that a "better" local approximation to the nonlocal potential defined in Ref. 17 can be obtained. Perey<sup>22</sup> has pointed out that one of the results coming from their study is that the values of the diffuseness of the real well differ from those values predicted by Eq. (35) in Ref. 17. Accordingly, we studied the effect of varying this parameter over a wide range. No substantial improvement in the agreement with the data was found. We hope to continue further work toward obtaining a more realistic optical potential for these nuclei in the energy range below 2 MeV.

#### ACKNOWLEDGMENTS

The authors wish to thank Dr. J. E. Monahan for useful discussions, D. Jordan for use of his subroutines for angular-momentum coupling coefficients, W. Ray, R. Amrein, and the crew of the Argonne 4.5-MeV Van de Graaff accelerator for their assistance in the experiment, and D. Mueller, R. Obenchain, B. Blumenstein, and C. Walker for aid in data reduction.

<sup>21</sup> F. G. Perey and D. S. Saxon (to be published).

<sup>22</sup> F. G. Perey (private communication).

## Thresholds for (*p,n*) Reactions on 26 Intermediate-Weight Nuclei\*

C. H. JOHNSON, C. C. TRAIL,† AND A. GALONSKY‡

*Oak Ridge National Laboratory, Oak Ridge, Tennessee*

(Received 12 August 1964)

Protons with energies below 5 MeV, produced by either a 3-MV or a 5.5-MV Van de Graaff accelerator, were used to find (*p,n*) thresholds and threshold limits for 26 nuclei with  $37 \leq A \leq 112$ . Data are presented from several independent measurements which were made over a period of about five years; the present values supersede those presented in earlier abstracts by Trail and Johnson and by Johnson and Galonsky. Energy calibrations are based on one or more of the following absolute standards: <sup>7</sup>Li(*p,n*), 1880.7±0.4 keV; <sup>11</sup>B(*p,n*) 3016.4±1.5; <sup>19</sup>F(*p,n*), 4234.4±1.0 keV; and <sup>19</sup>F(*p,αγ*), 872.5±0.4, 934.1±0.9, 1346.6±1.1, and 1373.5±0.6 keV. Neutrons were detected in each experiment by several BF<sub>3</sub> counters in 4π geometry. The yields near threshold have been interpreted in terms of the Hauser-Feshbach statistical theory of the compound nucleus, and in most cases there is good agreement with the predictions for the ground-state transitions. The targets and the corresponding negative *Q* values in keV for these ground-state transitions are as follows: <sup>37</sup>Cl, 1596.9±2.5; <sup>41</sup>K, 1209.7±1.5; <sup>49</sup>Ti, 1383.6±1.0; <sup>51</sup>V, 1533.7±1.8; <sup>53</sup>Cr, 1380.4±1.6; <sup>55</sup>Mn, 1014.4±0.8; <sup>57</sup>Fe, 1619±2; <sup>59</sup>Co, 1855.3±1.6; <sup>61</sup>Ni, 3024±4; <sup>65</sup>Cu, 2135.8±1.7; <sup>67</sup>Zn, 1783.3±1.4; <sup>68</sup>Zn, 3707±5; <sup>69</sup>Ga, 3006±4; <sup>70</sup>Zn, 1439±3; <sup>71</sup>Ga, 1018±2; <sup>74</sup>Ge, 3348±5; <sup>76</sup>As, 1647.3±1.1; <sup>80</sup>Se, 2653±3; <sup>106</sup>Pd, 3754±13; <sup>108</sup>Pd, 2670±100; and <sup>112</sup>Cd, 3400±20. In addition, three thresholds were observed for which the comparison of the observed yields with the predictions indicates that the reactions proceed to the excited states in the residual nuclei. The three targets and the corresponding negative *Q* values in keV are as follows: <sup>73</sup>Ge, 1189±15; <sup>89</sup>Y, 4207±6; <sup>93</sup>Nb, 2720±100. The fact that the <sup>93</sup>Nb(*p,n*)<sup>93</sup>Mo threshold to the 1.48-MeV state was observed indicates that lower states in <sup>93</sup>Mo have  $J \leq \frac{5}{2}$ . For three other targets the yield curves showed some indication of a threshold; however, comparisons with the theory in these cases indicate that only the following upper limits can be set to  $-Q$  in keV: <sup>48</sup>Ca(*p,n*)<sup>48</sup>Sc, <640; <sup>82</sup>Se(*p,n*)<sup>82</sup>Br, <920; <sup>93</sup>Nb(*p,n*)<sup>93</sup>Mo, <1290. A comparison with the theory indicates that the observed yield above 650 keV for <sup>48</sup>Ca must be due to a transition to an excited state rather than the ground state of <sup>48</sup>Sc.

### I. INTRODUCTION

THE mass difference between two isobars can often be found with ease and precision by observing the (*p,n*) reaction threshold for a ground-state tran-

sition. If the residual nucleus is unstable against positron emission, the negative of the *Q* value must be greater than 1804 keV; in this case the threshold energy

† Present address: Brooklyn College, Brooklyn, New York.

‡ Present address: Michigan State University, East Lansing, Michigan.

\* Research sponsored by the U. S. Atomic Energy Commission under contract with Union Carbide Corporation.

and the end point of the positron spectrum are independent data on the mass difference. If the residual nucleus is stable toward positron emission but unstable against  $K$  capture,  $-Q$  must lie between 782 and 1804 keV (these limits are found by neglecting the atomic binding of the  $K$  electron). The  $(p,n)$  threshold then contains information that is difficult to get by other means, but the threshold may be difficult to detect in intermediate weight nuclei because the low-energy protons must penetrate a high Coulomb barrier. Finally, in the rare case in which the target itself is unstable toward  $\beta^-$  decay,  $-Q$  must be less than the  $n-p$  mass difference of 782 keV. Thresholds in this low-energy region are extremely difficult to detect unless the target is a light nucleus such as  $^{14}\text{C}$  or tritium.

Our interest lies in the measurement of thresholds to a precision of a few keV for nuclei of intermediate weight,  $37 \leq A \leq 112$ . For these nuclei the threshold energy can be so far below the top of the Coulomb barrier that the ratio of yield to background is very small, and theoretical help may be required to interpret the data. It is well known<sup>1,2</sup> that, in an energy region that is small relative to the level spacing of the compound nucleus, the cross section just above threshold varies as  $E_n^{l+1/2}$  for outgoing  $l$ -wave neutrons of energy  $E_n$ ; however, this fact is useless here because the level spacings are usually less than the experimental energy uncertainty. For example, the observed<sup>3</sup> average spacing for the  $^{51}\text{V}(p,n)^{51}\text{Cr}$  reaction is less than 2 keV, and the spacings are probably smaller for most of the nuclei studied here. A useful theory is the Hauser-Feshbach<sup>4</sup> statistical treatment of the compound nucleus. Our earlier report<sup>5</sup> showed that this theory works well in a 500-keV interval just above threshold, and the present paper shows that the theory is useful even for an interval of only a few keV.

The compound-nucleus cross sections for the Hauser-Feshbach theory are calculated here, just as in the earlier report,<sup>5</sup> from a black-nucleus square-well potential rather than from a more realistic complex potential. The resulting values could be off by factors of 2 but are adequate for the present purpose. The important point is that the transmission of protons through the Coulomb barrier is so small that, once the compound nucleus is formed, it probably decays by  $\gamma$ -ray or neutron emission rather than by re-emission of the proton. If the conservation of parity and angular momentum permit neutrons of low  $l$  value, neutron emission quickly dominates as the energy goes above

threshold; hence, the  $(p,n)$  cross sections for channels which go by  $s$ -wave neutrons rise within 1 keV to their full compound-nucleus values. Even  $p$ -wave neutrons of a few keV compete favorably so that the cross sections for these channels rise within 10 or 20 keV to nearly their compound nucleus values. If the ground-state spin difference is 0 or 1, there are several open channels for  $s$ - or  $p$ -wave neutrons, and the total  $(p,n)$  cross section rises rapidly toward the total compound-nucleus value. The number of channels open to  $s$ - or  $p$ -wave neutrons is appreciable even for a ground-state spin difference of 2 because the proton has a relatively high probability of carrying in 1 or 2 units of orbital angular momentum. (For example, the  $s$ -,  $p$ -, and  $d$ -wave contributions by protons on  $^{51}\text{V}$  at the threshold are 43, 46, and 10%, respectively.) However, a threshold for a transition between ground states for which  $\Delta I \geq 3$  may be very difficult to detect.

The Hauser-Feshbach theory can help one to avoid mistakes. One mistake would be to assign a threshold to the energy at which the target yield first rises out of an excessive background. Errors of this type have appeared in the literature. A comparison with the theory would show that the observed cross section is essentially the compound-nucleus cross section, which rises rapidly with energy but not nearly so rapidly as does the  $(p,n)$  cross section at the threshold which was lost in the background at lower energy. Another mistake would be to confuse an excited-state threshold, involving a small spin difference, with a ground-state transition, which happens to be inhibited by a large spin difference. Another error would be to confuse the threshold for a target contaminant with that for the true target.

The actual cross section may have resonances that fluctuate widely from the predicted averages, so that, as pointed out by Schoenfeld *et al.*,<sup>6</sup> the first resonance in the  $(p,n)$  reaction may be mistaken for the true threshold. Some estimate of the possible error can be made by looking at the  $^{51}\text{V}(p,n)^{51}\text{Cr}$  yield curves which Gibbons *et al.*<sup>3</sup> obtained with an energy resolution of better than 1 keV. Pronounced resonances are present with spacings up to about 6 keV and with peak-to-valley ratios of about 10 or 20 near threshold. The experimental problem, if the threshold happens to be in a region of low cross sections between resonances, is basically to obtain an adequate ratio of signal to background. Consider for example the  $^{51}\text{V}(p,n)^{51}\text{Cr}$  threshold; our yield curve in Fig. 1 rises to 25 times background at 1 keV above threshold and to 250 times background at 3 keV, and this seems to be more than would be expected for a resonance. The rise at threshold for a heavier target, such as  $^{75}\text{As}$  in Fig. 1, is less spectacular because of the higher Coulomb barrier; but also the magnitude of the possible error is less because the levels are more closely spaced.

<sup>1</sup> J. M. Blatt and V. F. Weisskopf, *Theoretical Nuclear Physics* (John Wiley & Sons, Inc., New York, 1952), p. 396.

<sup>2</sup> J. B. Marion and T. W. Bonner, *Fast Neutron Physics*, edited by J. B. Marion and J. L. Fowler (Interscience Publishers Inc., New York, 1963), p. 1865.

<sup>3</sup> J. H. Gibbons, R. L. Macklin, and H. W. Schmitt, *Phys. Rev.* **100**, 167 (1955).

<sup>4</sup> W. Hauser and H. Feshbach, *Phys. Rev.* **87**, 366 (1952).

<sup>5</sup> C. H. Johnson, A. Galonsky, and J. P. Ulrich, *Phys. Rev.* **109**, 1243 (1958).

<sup>6</sup> W. A. Schoenfeld, R. W. Duborg, W. M. Preston, and C. Goodman, *Phys. Rev.* **85**, 873 (1952).

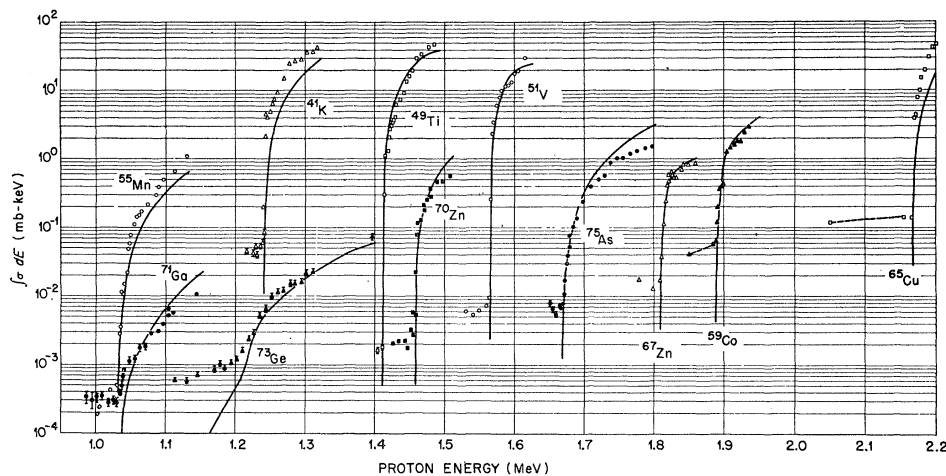


FIG. 1. Yields in mb-keV near thresholds for 11 targets from experiment A, specifically experiments denoted by  $A^a$  in Table II. For each target the observed yield has been multiplied by a constant such that, if the background is negligible, the ordinate is the integral  $\int \sigma dE$  of the ( $p, n$ ) cross section integrated over the target thickness. A constant factor was used even in the region of relatively high background near or below the threshold in order not to distort the shape of the yield curve. Theoretical curves are based on the Hauser-Feshbach theory for a black square-well nucleus of radius  $1.45 \times A^{1/3}$  F for transitions between the initial and final states with  $J^\pi$  as given in Table II. The thresholds were chosen to fit the theory to the experiment. The agreement of the theoretical and experimental yields, each of which has about a  $\pm 50\%$  uncertainty, indicates that the thresholds have been assigned to the correct transitions. In particular the threshold for the  $^{73}\text{Ge}$  target is assigned to a transition to the  $\frac{5}{2}^-$  excited state in  $^{73}\text{As}$ .

Brugger, Bonner, and Marion<sup>7</sup> also emphasized the possibility of such an error and Marion and Kavanagh<sup>8</sup> later found the  $^{65}\text{Cu}(p, n)^{65}\text{Zn}$  threshold about 5 keV lower than reported previously<sup>7,9</sup> but in agreement with several measurements of the  $^{65}\text{Zn}$  positron end point. They suggested that the earlier thresholds might contain this type of error; however, the present result and that of Okano and Nishimura<sup>10</sup> both were obtained with good signal-to-noise ratios, and both agree with the old higher values but disagree, outside the quoted errors, with the value of Marion and Kavanagh. A good measurement of the neutron energy would resolve the discrepancy.

The most likely situation for confusing a resonance with a threshold would be in a relatively light intermediate nucleus in which the levels are widely spaced while, at the same time, the cross section is reduced because of a large spin difference between the ground states. Thus, Parks *et al.*<sup>11</sup> found the threshold for  $^{37}\text{Cl}(p, n)^{37}\text{K}$ , for which  $\Delta I = 0$ , to agree with the  $Q$  value determined by measuring the outgoing neutron energy, but the threshold for  $^{40}\text{A}(p, n)^{40}\text{K}$ , for which  $\Delta I = 4$ , to be 3 keV higher than that derived from the neutron energy measurements. This seems to be the only experi-

ment in which both the neutron energy and the threshold have been measured with sufficient precision to make a careful comparison, and the fact that only a 3-keV error occurred for the extreme case of  $\Delta I = 4$  is encouraging. It is also encouraging that there are many threshold measurements in the literature which were obtained with rather poor signal-to-background ratios and yet agree with the present results. Apparently, thresholds are easier to observe than one might think. We cannot be certain that a "resonance" error does not exist in our work; but certainly our good signal-to-background ratios reduce the chance for the error. Our quoted uncertainties include no estimate of the effect.

This paper reports thresholds for protons of less than 5 MeV on intermediate nuclei,  $37 \leq A \leq 112$ , for three independent sets of measurements which were made over a period of several years. The first set of measurements (experiment A) was taken primarily to find thresholds below 1.8 MeV and was partially reported in an abstract by Trail and Johnson.<sup>12</sup> Results reported here differ from those in the published abstract primarily because the energy calibration standards have since changed. Results are also given which did not appear in the abstract. The second set (experiment B) was primarily a study of proton strength functions, which has been published,<sup>5</sup> but also included new measurements of known thresholds, which are given here. The third set (experiment C) includes several thresholds, which Johnson and Galonsky<sup>13</sup> gave in an abstract,

<sup>7</sup> R. M. Brugger, T. W. Bonner, and J. B. Marion, *Phys. Rev.* **100**, 84 (1955).

<sup>8</sup> J. B. Marion and R. W. Kavanagh, *Phys. Rev.* **104**, 107 (1956).

<sup>9</sup> J. D. Kingston, J. K. Bair, H. O. Cohn, and H. B. Willard, *Phys. Rev.* **99**, 1393 (1955).

<sup>10</sup> K. Okano and K. Nishimura, *J. Phys. Soc. Japan* **18**, 1563 (1963).

<sup>11</sup> P. B. Parks, P. M. Beard, E. G. Bilpuch, and H. W. Newson, *Bull. Am. Phys. Soc.* **9**, 32 (1964).

<sup>12</sup> C. C. Trail and C. H. Johnson, *Phys. Rev.* **91** 474A (1953).

<sup>13</sup> C. H. Johnson and A. Galonsky, *Bull. Am. Phys. Soc.* **5**, 443 (1960).

and also new measurements of known thresholds; the values given here for this set differ slightly from the abstract values. Since our older values have been included in reviews such as the Nuclear Data Sheets,<sup>14</sup> it is important to state clearly that *values reported here supersede those from the abstracts of Trail and Johnson<sup>12</sup> and of Johnson and Galonsky.<sup>13</sup>*

## II. MEASUREMENTS

### 1. General Method

The experiments A, B, and C were similar. In each case protons from an electrostatic accelerator were analyzed by a magnet which was calibrated in terms of a magnetic resonance device against the energy standards in Table I. The proton charge collected on the

TABLE I. Energy standards for experiments A, B, and C.

Experiment	Reaction	Resonance or threshold (keV)	Basis of standard
A	$^{19}\text{F}(p,\alpha\gamma)^{16}\text{O}$	$872.5 \pm 0.4^a$	Absolute
		$934.1 \pm 0.9^b$	Absolute
		$1346.6 \pm 1.1^a$	Absolute
		$1373.5 \pm 0.6^a$	Absolute
		$1880.7 \pm 0.4^a$	Absolute
B	$^7\text{Li}(p,n)^7\text{Be}$	$1564.4 \pm 1.1^{c,d,e}$	Rel. to $^7\text{Li}(p,n)$ and $^{19}\text{F}(p,\alpha\gamma)$
	$^{51}\text{V}(p,n)^{51}\text{Cr}$		
C	$^{37}\text{Cl}(p,n)^{37}\text{A}$	$1640 \pm 1^f$	Rel. to $^7\text{Li}(p,n)$
	$^{11}\text{B}(p,n)^{11}\text{C}$	$3016.4 \pm 1.5^g$	Absolute
	$^{19}\text{F}(p,n)^{19}\text{Ne}$	$4234.4 \pm 1.0^{g,h}$	Absolute

<sup>a</sup> J. B. Marion, Ref. 17.

<sup>b</sup> Hunt *et al.*, Ref. 18. We reduced the 935.1-keV value of Hunt and Firth by 1 keV because Hunt *et al.* found the other resonances about 1 keV lower than those of Hunt and Firth.

<sup>c</sup> Gibbons *et al.*, Ref. 3. Their value of 1565.6 is reduced to 1565.0 on the basis of the newer  $^7\text{Li}(p,n)$  standard.

<sup>d</sup> Gossett and Butler, Ref. 23.

<sup>e</sup> Experiment A, this report.

<sup>f</sup> Parks *et al.*, Ref. 11.

<sup>g</sup> E. H. Beckner, R. L. Bramblett, G. C. Phillips, and T. A. Eastwood, Phys. Rev. 123, 2100 (1961).

<sup>h</sup> A. Rytz, H. Winkler, F. Zamboni, and W. Zych, Helv. Phys. Acta 34, 819 (1961).

target was measured by a current integrator, and the neutrons were detected by several  $\text{BF}_3$  counters imbedded in paraffin or graphite in an approximate  $4\pi$  geometry. This arrangement was chosen in preference to the forward geometry, which is usually used for lighter nuclei, because the neutron yields from intermediate weight nuclei become distributed over  $4\pi$  sr within 1 keV above threshold. The arrangement is efficient and allows for easy shielding against external background. Backgrounds were minimized by placing the target several feet from the analyzing magnet and by using clean Pt or Ta beam-defining apertures. A liquid-nitrogen trap reduced carbon buildup on the target.

Table II lists the target isotopes for all three experiments. The initial and final state values of  $J^\pi$ , which are

<sup>14</sup> Nuclear Data Sheets, compiled by K. Way *et al.* (Printing and Publishing Office, National Academy of Sciences—National Research Council, Washington 25, D. C.), (through 1963).

taken from the 1958–61 Nuclear Data Sheets, are known or fairly well established unless they are enclosed in parenthesis. Excited states are also tabulated for the final nuclei produced by protons on  $^{73}\text{Ge}$ ,  $^{89}\text{Y}$  and  $^{93}\text{Nb}$ . Columns 5–7 give the isotopic abundances, chemical forms, and thicknesses in keV at threshold or at the limit to the threshold. Most targets are listed only once; however, two of them ( $\text{TiO}_2$  and  $\text{ZnO}$ ) are each listed twice because they were used for separate measurements. Two thick targets, Ti and Nb, were disks of the natural elements, but the others were made by evaporation or electrodeposition of the element or a compound (usually enriched<sup>15</sup> in the target isotope) onto 1.25-in.-diam disks of platinum (sometimes gold). These backings were chosen because they give low  $(p,n)$  yields at these energies and are easy to clean by scrubbing with an eraser, washing with solvents, and flaming. Care was taken in preparing the targets to avoid contaminants that might obscure the thresholds. Targets for experiments A and B were prepared by evaporation from tantalum or tungsten filaments which had been cleaned by preheating in vacuum; a shutter shielded each disk except during the actual evaporation. The  $\text{CaO}$  target was formed by evaporation, and also decomposition, of  $\text{CaCO}_3$ , but the other targets of compounds are assumed to have been formed without decomposition during the evaporation. Most targets for experiment C were electroplated by E. B. Olszewski in the Isotope Division at Oak Ridge.

### 2. Experiment A

These measurements were made in 1952 primarily to find thresholds in the region below 1.8 MeV where the presence of the Coulomb barrier creates an intensity problem but where the results are particularly valuable because they afford a simple determination of mass differences that are difficult to obtain by other means. The 3-MV Van de Graaff<sup>16</sup> used here was well suited because it delivered up to 100  $\mu\text{A}$  of protons. It also had very good energy resolution,  $<0.025\%$ , due to a control circuit which R. F. King designed to be used in conjunction with the 90-deg analyzing magnet. Calibration of the magnet was made with a deuterium magnetic-resonance fluxmeter in terms of the  $^7\text{Li}(p,n)$  threshold and several  $^{19}\text{F}(p,\alpha\gamma)$  resonances as indicated in Table I. Experiment A actually consists of five subgroups which were generally separated by several months during which changes in the accelerator were made. A fresh thin  $^{19}\text{F}$  target was made for each subgroup by exposing a tantalum disk briefly to HF fumes, and the  $\gamma$  rays produced by the protons on the target were detected in a  $\text{NaI}(\text{TI})$  crystal; the calibration was accepted if the observed resonance widths were consistent with the

<sup>15</sup> Separated isotopes prepared by the Stable Isotope Division at Oak Ridge National Laboratory.

<sup>16</sup> C. H. Johnson, J. P. Judish, and C. W. Snyder, Rev. Sci. Instr. 28, 942 (1957).

TABLE II. Targets and observed thresholds for experiments A, B, and C. The target thickness is given at the threshold energy. Values of  $J^\pi$  are taken from the Nuclear Data Sheets. The  $J^\pi$  assignments which are enclosed in parenthesis are uncertain, whereas the others are either known or highly probable values.

Target nucleus	Initial $J^\pi$	Final $J^\pi$	Experiment	Isotopic abundance (percent)	Chemical form	Target thickness (keV)	Threshold (keV)
<sup>37</sup> Cl	$\frac{3}{2}^+$	$\frac{3}{2}^+$	B	24.5	NaCl	26	1640.5±2.5
<sup>41</sup> K	$\frac{3}{2}^+$	$\frac{3}{2}^-$	A	6.9	KCl	73	1239.5±1.5
<sup>48</sup> Ca	$0^+$	$6^+$	A	84.3	CaO	50	<650
<sup>49</sup> Ti	$\frac{7}{2}^-$	$\frac{7}{2}^-$	A	5.51	Ti	Thick	1412.7±2.5
			A	77.6	TiO <sub>2</sub>	39	1409.6±2.5
			A	77.6	TiO <sub>2</sub>	48	1412.5±2.0
			B	5.5	Ti	18	1410.6±1.9
			C	77.6	TiO <sub>2</sub>	48	1415.7±2.5
<sup>51</sup> V	$\frac{7}{2}^-$	$\frac{7}{2}^-$	A	99.8	V <sub>2</sub> O <sub>5</sub>	27	1564.1±1.8
<sup>58</sup> Cr	$\frac{3}{2}^-$	$\frac{7}{2}^-$	B	9.55	Cr	16	1405.1±2.1
			C	96.5	Cr	210	1409 ±2.5
<sup>55</sup> Mn	$\frac{5}{2}^-$	$\frac{3}{2}^-$	A	100	Mn	>120	1034.5±2.1
			A	100	Mn	>120	1033.9±1.3
			A <sup>a</sup>	100	Mn	145	1033.0±1.7
			B	100	Mn	15	1030.6±1.6
<sup>57</sup> Fe	$\frac{1}{2}^-$	$\frac{7}{2}^-$	C	84.1	Fe	40	1648 ±2
<sup>59</sup> Co	$\frac{5}{2}^-$	$\frac{3}{2}^-$	A	100	Co	22	1887.3±1.8
			B	100	Co	24	1886.9±3.1
<sup>61</sup> Ni	$\frac{3}{2}^-$	$\frac{3}{2}^-$	C	85.0	Ni	120	3074 ±4
<sup>65</sup> Cu	$\frac{3}{2}^-$	$(\frac{3}{2}^-)$	A	30.9	Cu	140	2169.7±2.1
			B	30.9	Cu	19	2167.5±3.2
<sup>67</sup> Zn	$\frac{5}{2}^-$	$\frac{3}{2}^-$	A <sup>a</sup>	60.5	ZnO	9	1810.6±2.5
			A	60.5	ZnO	9	1809.3±2.5
			C	57.2	Zn	120	1810.7±2.2
<sup>68</sup> Zn	$0^+$	$1^+$	C	96.8	Zn	62	3762 ±5
<sup>69</sup> Ga	$\frac{3}{2}^-$	$(\frac{3}{2}^- \text{ or } \frac{3}{2}^-)$	C	98.1	Ga	88	3050 ±4
<sup>70</sup> Zn	$0^+$	$1^+$	A	48.4	ZnO	unknown	1462 ±3
			A <sup>a</sup>	48.4	ZnO	260	1454 ±5
<sup>71</sup> Ga	$\frac{3}{2}^-$	$\frac{1}{2}^-$	A <sup>a</sup>	39.6	Ga	220	1033 ±4
			A	39.6	Ga	30	1035 ±4
			A	98.1	Ga <sub>2</sub> O	31	1036 ±5
			B	39.6	Ga	23	1031 ±3
<sup>78</sup> Ge	$\frac{9}{2}^+$	$\frac{3}{2}^-, \frac{5}{2}^-$ <sup>b</sup>	A	78.0	GeO	29	1205 ±15 <sup>b</sup>
<sup>74</sup> Ge	$0^+$	$2^-$	C	97.7	Ge	16	3394 ±5
<sup>76</sup> As	$\frac{3}{2}^-$	$\frac{5}{2}^+$	A	100	As	11	1669.6±2.4
			A <sup>a</sup>	100	As	50	1669.7±1.7
			B	100	As	21	1669.1±1.9
<sup>80</sup> Se	$0^+$	$1^+$	C	98.4	Se	24	2686 ±3
<sup>82</sup> Se	$0^+$	$5^-$	B	75.7	Se	17	<930
<sup>89</sup> Y	$\frac{1}{2}^-$	$(\frac{9}{2}^+), (\frac{1}{2}^-)$ <sup>b</sup>	C	100	Y	26	4255 ±6 <sup>b</sup>
<sup>93</sup> Nb	$\frac{9}{2}^+$	$(\frac{5}{2}^+)$	B	100	Nb	thick	<1300
	$\frac{9}{2}^+$	$(\frac{9}{2}^+)$ <sup>b</sup>	C	100	Nb	thick	2750 ±100 <sup>b</sup>
<sup>106</sup> Pd	$0^+$	$1^+$	C	82.3	Pd	36	3790 ±13
<sup>108</sup> Pd	$0^+$	$1^+$	C	94.7	Pd	68	2700 ±100
<sup>112</sup> Cd	$0^+$	$1^+$	C	96.5	Cd	60	3430 ±20

<sup>a</sup> Figure 1 shows yield curves for these subgroups of experiment A.

<sup>b</sup> Excited-state thresholds.

known natural widths.<sup>17,18</sup> Several energy standards were required because the fluxmeter frequency was not read directly but rather in terms of a dial setting on a tuning condenser. The resulting calibration points showed that the frequency varied linearly with the dial setting, and a combined calibration constant for each subgroup was found from the best fit with relativistic corrections to the several energy standards.

Neutrons produced by the protons incident on the water-cooled target were detected in three 1-in.-diam BF<sub>3</sub> counters which nearly surrounded the target. Each

counter was enclosed by a  $\frac{3}{4}$ -in.-thick layer of paraffin in order to increase the sensitivity to neutrons of a few keV energy, and the entire array was shielded on all sides by about 1-ft thickness of borated water. The efficiency for PoBe neutrons was approximately 1%, and, although an efficiency measurement was not made in the low-energy region of interest, a comparison of the yield curves to the absolute cross sections of experiment B shows that the efficiency was about 1% in this region also. A constant efficiency of 1% will be assumed for the following discussion. This is a crude approximation (undoubtedly there was some energy dependence and the average could be 0.5 to 1.5%), but it is good enough for the intercomparison of yields in limited regions near thresholds.

<sup>17</sup> J. B. Marion, Rev. Mod. Phys. 33, 139 (1961).

<sup>18</sup> S. E. Hunt and K. Firth, Phys. Rev. 99, 786 (1955) and S. E. Hunt, R. A. Pope, D. V. Freck, and W. W. Evans, *ibid.* 120, 1740 (1960).

Figure 1 presents yields for the 11 targets whose thresholds were found in experiment A; if more than one curve was obtained for a given isotope, the one shown is from the subgroup denoted by A<sup>a</sup> in Table II. It is worth noting that a clearer presentation would have been given by two very similar figures, the first of which would show simply the counts/Coulomb versus proton energy and would demonstrate that each yield rises abruptly at threshold out of a slowly rising background. The second figure would then compare the predictions of the statistical theory with the observed cross section, which would be corrected for background and be plotted at the average energy in the target. Figure 1 is intended to be a space-saving compromise in which the yields, including backgrounds, are plotted versus the bombarding proton energy, but also a comparison is made to the theory. Each yield has been multiplied by a constant in order to convert to units of mb-keV, i.e.,

$$\left( \int \sigma dE \right)_{\text{observed}} = (1.6 \times 10^{-6} S/P)(Y/e), \quad (1)$$

where  $Y$  is the observed yield in counts/C,  $e$  is the detector efficiency in percent,  $P$  is the percentage isotopic abundance, and  $S$  is the stopping power<sup>19</sup> in  $10^{-18}$  keV-cm<sup>2</sup>/atom.

In the regions above thresholds, where the backgrounds are negligible, the resulting ordinate is the cross section integrated over the effective target thickness. Note that the shape of each yield curve has not been changed by the multiplication by a constant but that the curves for the targets with low isotopic abundance are shifted upward relative to the enriched targets. For example, the curve for <sup>41</sup>K in the figure is shifted so that its background appears abnormally high.

The solid curves in Fig. 1 show  $\int \sigma dE$ , where  $\sigma$  is the  $(p,n)$  cross section derived from the statistical theory of the compound nucleus<sup>4,5</sup> for a black square-well potential of radius  $R=1.45A^{1/3}$  f, and the integration is over the target thickness (above threshold). Initial and final values of  $J^\pi$  for the calculation are listed in Table II. The only adjustable parameters are the thresholds, which were chosen to fit the data.

The agreement between theory and experiment is gratifying considering the facts that the statistical theory is only an average approximation, that the black-nucleus potential is not completely realistic, and that the observed cross sections have uncertainties of perhaps a factor of 2. It seems clear from the comparison with theory that each threshold has been assigned to the correct transition. Of course, some of the thresholds, such as those for <sup>49</sup>Ti and <sup>51</sup>V, are so pronounced that one need not bother with the theory; but others are

less dramatic and are more readily interpreted in this way.

Two cases are noteworthy. The first is the <sup>71</sup>Ga( $p,n$ ) threshold which happens to be at the same energy as that for <sup>55</sup>Mn( $p,n$ ) and could conceivably have arisen from a 1% contaminant of <sup>55</sup>Mn. A spectroscopic analysis ruled out this possibility, but also the observed shape and magnitude of the yield curve agrees nicely with the theory for <sup>71</sup>Ga. The other noteworthy yield is that for <sup>73</sup>Ge( $p,n$ )/<sup>73</sup>As, which rises out of the background at about 1205 keV and shows a change in slope on the semilog plot at about 1250 keV. The change in slope is important; for, if it were not present, one could attribute the yield to a threshold far below 1205 keV. The ground state transition,  $\frac{9}{2}^+$  to  $\frac{3}{2}^-$ , requires  $l$  waves too high to account for the observed shape and magnitude of the yield. There is, however, a 66-keV excited state in <sup>73</sup>Ge which has been assigned<sup>14</sup>  $\frac{5}{2}^-$ ; and this transition, along with the ground-state transition, gives the theory shown for a  $(1205 \pm 15)$ -keV excited state threshold. Actually, our measurements cannot tell whether this  $\frac{9}{2}^-$  to  $\frac{5}{2}^-$  threshold is to the excited or the ground state; however, we assign it to the excited state in accordance with the Nuclear Data Sheets.

Threshold energies derived from these yield curves and from other independent subgroups for experiment A are given in the last column of Table II. The theory discussed here was helpful for assigning the threshold energies; but actually they were usually taken to be at the energy where the yield first rises out of the background. The assigned standard errors are a statistical combination of the following: (1) uncertainties in the standards in Table I, (2) estimated uncertainties in locating the resonances or threshold for calibration, and (3) estimated uncertainty in locating the threshold in the yield curve for the target.

Our measurements on <sup>48</sup>Ca( $p,n$ )/<sup>48</sup>Sc are of considerable interest even though they establish only an upper limit to the threshold. Figure 2 shows the yield curve; the indicated background was observed from a clean Pt blank. At 650 keV the CaO target thickness was 50 keV, and we note (with pride) that the minimum observed cross section is about  $2 \times 10^{-6}$  mb. No clearly defined threshold, such as those in Fig. 1, is observed and there seems to be no valid basis for extrapolating to a "threshold" at 650 keV. A valid statement is that the threshold is below 650 keV and that the data are consistent with the  $(-660 \pm 30)$ -keV  $Q$  value observed by Elwyn *et al.*<sup>20</sup> by neutron time-of-flight.

The theoretical curve in Fig. 2 is  $\int \sigma_e dE$ , where  $\sigma_e$  is the cross section for formation of the compound nucleus for a black square-well potential. One would expect the  $(p,n)$  cross section to approach this curve, but actually the theory lies at least a factor of 20 above the observed yield. The reason is not clear. Both the theory and the

<sup>19</sup> Ward Whaling, *Encyclopedia of Physics*, edited by S. Flügge (Springer-Verlag, Heidelberg, 1958), Vol. 34, p. 193.

<sup>20</sup> A. J. Elwyn, H. H. Landon, S. Oleksa, and G. N. Glasoe, *Phys. Rev.* **112**, 1200 (1958).

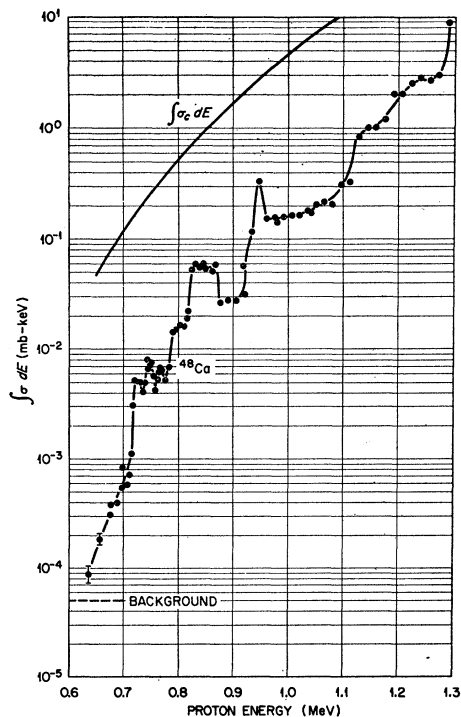


FIG. 2. Yield in mb-keV from experiment A for the  $^{48}\text{Ca}(p,n)^{48}\text{Sc}$  reaction for a target that was 50-keV thick at 650 keV. The indicated background was observed on a clean Pt blank. The smooth curve is the predicted yield for compound-nucleus formation for a black square-well potential. A detailed discussion of the poor agreement between the theory and the experiment is not warranted because of the large uncertainties in both curves; nevertheless, the conclusion is made that the yield does not result from the ground-state ( $0^+$  to  $6^+$ ) transition and that the threshold is below 650 keV.

observed yield could easily be off by factors of 2; nevertheless, a discrepancy would still exist. Perhaps all available states in the residual  $^{48}\text{Sc}$  nucleus require a large spin change so that the ( $p, n$ ) cross section is much smaller than  $\sigma_c$ . Certainly the observed yield is due to  $^{48}\text{Ca}$  because no target contaminant could give an appreciable yield at these energies. In any case it appears certain that the observed yield for  $^{48}\text{Ca}$  is not due to the  $0^+$  to  $6^+$  ground-state transition because predictions from the statistical model give only  $3 \times 10^{-9}$  mb-keV at 700 keV, a factor of  $10^6$  smaller than observed. Thus the  $Q$  value of  $-660 \pm 30$  keV, which Elwyn *et al.*<sup>20</sup> assigned to the ground state, should be assigned to a transition to a  $^{48}\text{Sc}$  excited state. Way<sup>21</sup> also concluded that this is not the ground state transition because mass spectroscopic data<sup>22</sup> indicate that the ground state  $Q$  is  $-520 \pm 20$  keV. Her conclusion that the  $Q$  of  $-660$  keV leads to a state of fairly high spin (say  $4^+$ ) is consistent with the low yield observed here.

<sup>21</sup> *Nuclear Data Sheets*, compiled by K. Way *et al.* (Printing and Publishing Office, National Academy of Sciences—National Research Council, Washington 25, D. C., 1961), NRC 61-2-4.

<sup>22</sup> C. F. Giese and J. L. Benson, *Phys. Rev.* **110**, 712 (1958).

### 3. Experiment B

Most of experiment B was described in our paper on proton strength functions.<sup>5</sup> The accelerator and magnetic analyzer were the same as in experiment A except that the protons were bent only 60 deg and a newer magnetic resonance fluxmeter was used with provisions for measurement of the resonance frequencies. Neutrons produced by ( $p, n$ ) reactions were detected with known efficiency by several  $\text{BF}_3$  counters clustered closely about the target and imbedded in a block of paraffin. The  $^{51}\text{V}(p, n)$  reaction served as the energy standard and also as a variable energy neutron source during the process of finding the detector's efficiency curve. The standard threshold,  $1564.4 \pm 1.1$  keV, in Table I is based on the results of experiment A and on two other values<sup>3,23</sup> each adjusted in accordance with the more recent  $^7\text{Li}(p, n)$  threshold in Table I. Several measurements of the  $^{51}\text{V}(p, n)$  threshold during the course of experiment B showed it to be reproducible to  $\pm 1$  keV.

Table II lists the thresholds observed for targets of  $^{37}\text{Cl}$ ,  $^{49}\text{Ti}$ ,  $^{53}\text{Cr}$ ,  $^{55}\text{Mn}$ ,  $^{59}\text{Co}$ ,  $^{65}\text{Cu}$ ,  $^{71}\text{Ga}$ , and  $^{75}\text{As}$ , all of which had been found earlier in experiment A or had been reported in the literature. The yield curves are quite similar to those in Fig. 1 and the error assignments have been made as in experiment A. One new threshold, that for  $^{77}\text{Se}(p, n)^{77}\text{Br}$ , was found and reported in our earlier paper.<sup>5</sup>

Experiment B included two cases,  $^{82}\text{Se}(p, n)^{82}\text{Br}$  and  $^{93}\text{Nb}(p, n)^{93}\text{Mo}$ , for which we assign only upper limits to the thresholds. These are cases where comparison with the theoretical cross section prevents one from erroneously assigning thresholds at 0.93 and 1.25 MeV, respectively. Figure 3 shows the yields, again in units of mb-keV, and shows the background levels near the lower limits for each curve. The shape of the  $^{82}\text{Se}(p, n)$  yield is the same as that predicted for the formation of the compound nucleus, whereas, if a threshold were clearly present, the experimental yield should fall faster than the compound-nucleus cross section as the energy decreases toward threshold. Thus, only an upper limit of 930 keV is assigned.

A theoretical curve for  $^{93}\text{Nb}(p, n)$  is not given because it cannot be plotted uniquely for a thick target. Cross section curves shown in our report<sup>5</sup> could possibly be interpreted to show that a threshold occurs near 1280 keV in agreement with the  $Q$  value found by Patterson,<sup>24</sup> but we prefer to assign only an upper limit, 1300 keV. In any case, if an assignment were made on the basis of these data, it should not rely only on extrapolation to an apparent zero yield but should also make use of the predicted shape of the yield curve.

### 4. Experiment C

The main purpose of C was to extend the study of proton strength functions to higher energies and mass

<sup>23</sup> C. R. Gossett and J. W. Butler, *Phys. Rev.* **113**, 246 (1959).

<sup>24</sup> R. Patterson, *Phys. Rev.* **95**, 303A (1954).

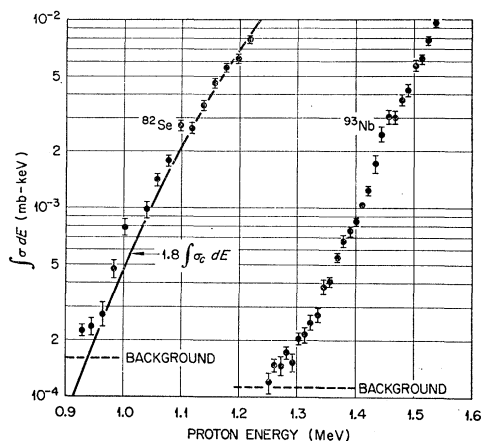


FIG. 3. Yields in mb-keV from experiment B for a thick  $^{83}\text{Nb}$  target and for a  $^{82}\text{Se}$  target that was 17 keV thick at 930 keV. Backgrounds are indicated as observed for clean Pt blanks. The predicted yield, multiplied by 1.8, is shown for formation of the compound nucleus by protons on  $^{82}\text{Se}$ . If a threshold for the  $^{82}\text{Se}(p,n)^{83}\text{Br}$  reaction were clearly present, the observed yield at the threshold would drop sharply below the theoretical curve. Thus the data allow only the assignment of threshold limits, <930 keV for  $^{82}\text{Se}$  and <1300 keV for  $^{83}\text{Nb}$ .

numbers. Protons were produced by a 5.5-MV accelerator and analyzed by a 90-deg magnet, identical to the one used above, calibrated relative to the  $^{11}\text{B}(p,n)$ ,  $^{37}\text{Cl}(p,n)$ , and  $^{19}\text{F}(p,n)$  thresholds listed in Table I. Here, unlike A and B, the magnet was driven close to saturation so that, because of nonuniformities in the iron, the fluxmeter did not measure the correct average field. This has two effects. Firstly, the calibration "constant" has a slight but well-established<sup>9</sup> energy dependence, and secondly, the calibration can change if the magnet is not properly cycled on a given hysteresis loop. Since we were not aware of this second problem at the time of the measurements, we have included a hysteresis uncertainty of  $\pm 0.1\%$ , based on later measurements, in each error estimate. This uncertainty is consistent with the measurements of the three calibration thresholds.

The  $4\pi$  neutron detector<sup>25</sup> was a five-foot sphere of graphite with several  $\text{BF}_3$  counters imbedded near its surface. Its flat response with known efficiency (about 3%) made it ideal for the measurement of absolute cross sections; however, its sensitivity to external neutron sources handicapped the measurements of thresholds. A low background was obtained by covering the sphere with cadmium and by removing most external sources. Fourteen thresholds were observed. Yield curves for three of these ( $^{49}\text{Ti}$ ,  $^{53}\text{Cr}$ , and  $^{67}\text{Zn}$ ) are similar to those from experiments A or B and will not be shown.

Of the eleven other thresholds, that for  $^{57}\text{Fe}(p,n)^{57}\text{Co}$  is particularly interesting because the ground-state transition has a large spin difference,  $\Delta I=3$ ; and no

<sup>25</sup> R. L. Macklin, Nucl. Instr. 1, 335<sup>2</sup>(1957).

levels in  $^{57}\text{Co}$  are known<sup>14</sup> below 1.37 MeV. The yield near threshold is reduced because of the large spin change; nevertheless, since the background was small, the threshold was clearly observed. As shown in Fig. 4 the yield rose within a 3-keV interval to 25 times background. The Hauser-Feshbach prediction for a black-nucleus approximation is consistent with the observed yield. At 7 keV above threshold this theory attributes 58% of the cross section to  $d$ -wave protons going to  $s$ -wave neutrons, 36% to  $p$ -wave protons going to  $p$ -wave neutrons, and a total  $(p,n)$  cross section of only 11% of the compound nucleus value. The fact that the actual yield rises faster than the theory is probably due to local  $d$ -wave resonances, and this particular threshold is probably the one most likely to have an error because of the resonance effect discussed in the introduction.

Figure 5 shows the counts/C versus proton energy near threshold for eight of the targets. The corresponding cross section curves (not given here) show that each curve rises to within a factor of 2 of the compound-nucleus cross section for a black nucleus. Backgrounds result from other isotopes or contaminants such as  $^{37}\text{Cl}$ . For each of the five lighter nuclei,  $^{61}\text{Ni}$ ,  $^{68}\text{Zn}$ ,  $^{69}\text{Ga}$ ,  $^{74}\text{Ge}$ , and  $^{80}\text{Se}$ , the position of the threshold and the characteristic shape of the yield curve is clearly de-

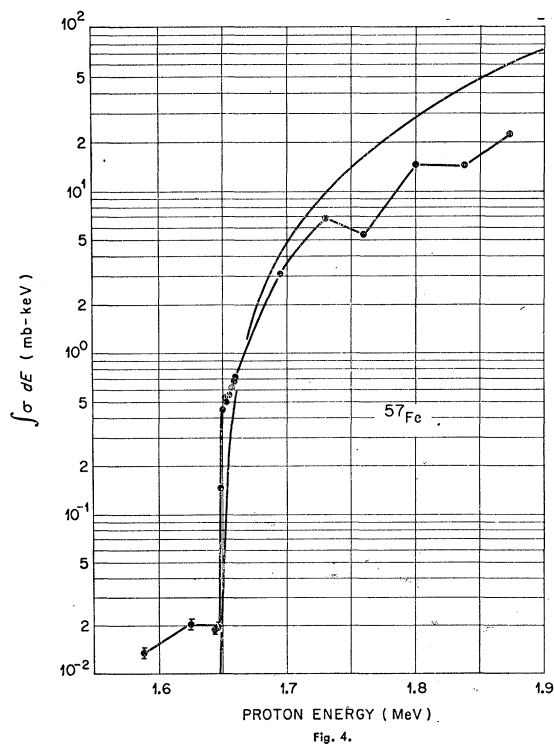


FIG. 4. Yield in mb-keV from experiment C for a  $^{57}\text{Fe}$  target that was 40 keV thick at the threshold. The smooth curve is the yield predicted for the  $(p,n)$  reaction for the ground-state ( $\frac{1}{2}^-$  to  $\frac{3}{2}^-$ ) transition. The theoretical and experimental curves show good agreement and demonstrate that, even though this is a transition with  $\Delta I=3$ , the background is low enough to allow the threshold to be observed. The threshold is  $1648 \pm 2$  keV.



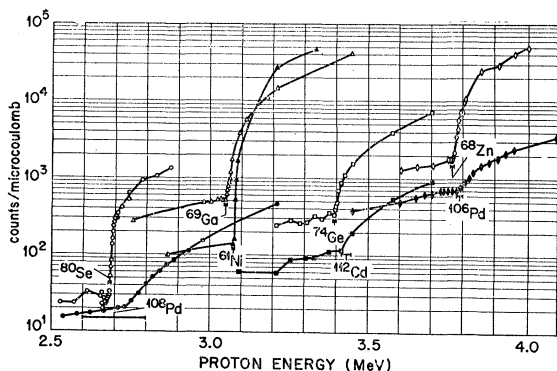


FIG. 5. Yields in counts/ $\mu$ C for eight targets from experiment C. Thresholds for the five lighter targets are clearly defined whereas those for  $^{106}\text{Pd}$ ,  $^{108}\text{Pd}$ , and  $^{112}\text{Cd}$  require further discussion (see Figs. 6 and 7).

finer; however, for the three heavier nuclei, the thresholds are more obscure and should be examined more closely. One approach would be to find ratios of the cross sections to those predicted for the formation of the compound nucleus; the presence of a threshold would be evidenced by a sharp drop of the experiment below the theory. The equivalent approach, which we have used, is to find the ratio of the observed cross sections to those for the heaviest isotope of the element. The heaviest isotope, being rich in neutrons, has a very low threshold so that its ( $p, n$ ) cross section is very nearly equal to the compound-nucleus cross section in the region of interest here. Figure 6 shows the cross sections for two lighter Pd isotopes relative to that observed for  $^{110}\text{Pd}$ ; clearly defined thresholds are seen for  $^{106}\text{Pd}$  and  $^{108}\text{Pd}$ . Figure 7 is a similar curve showing the threshold for  $^{112}\text{Cd}$ . In both figures, the random fluctuations for energies below about 3 MeV are the result of uncertainties in the subtraction of background.

Figure 8 shows the yield in arbitrary units for the excited-state thresholds of  $^{89}\text{Y}(p, n)^{89}\text{Zr}^*$  and  $^{93}\text{Nb}(p, n)^{93}\text{Mo}^*$ . Unfortunately, the  $^{89}\text{Y}$  target has a contaminant of  $^{37}\text{Cl}$  as evidenced by the comparison of

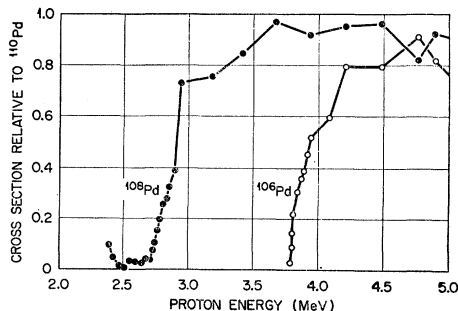


FIG. 6. Ratios of the cross sections for the  $^{106}\text{Pd}(p, n)$  and  $^{108}\text{Pd}(p, n)$  reactions to those observed for the  $^{110}\text{Pd}(p, n)$ . Essentially, these curves show the ratio of the ( $p, n$ ) cross sections to the cross sections for formation of the compound nucleus; and, being linear plots, show the thresholds clearer than the semilog plots of Fig. 5. The spurious yield below the  $^{108}\text{Pd}(p, n)$  threshold results from uncertainties in the background subtraction.

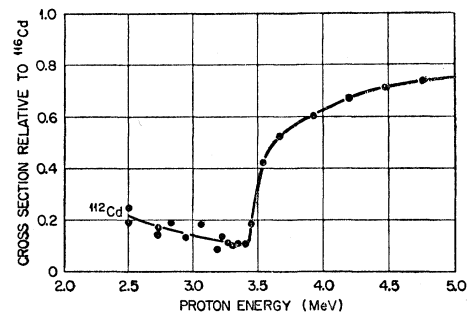


FIG. 7. Ratios of the  $^{112}\text{Cd}(p, n)$  cross sections to those observed for  $^{116}\text{Cd}(p, n)$ . Essentially, this shows the ratio of the  $^{112}\text{Cd}(p, n)$  cross section to that for formation of the compound nucleus; and, being a linear plot, it shows the threshold better than the semilog plot of Fig. 5. The spurious yield below 3.4 MeV results from uncertainties in the subtraction of backgrounds.

the  $^{37}\text{Cl}(p, n)$  yield (arbitrarily normalized) to the low-energy part of the yield from the  $^{89}\text{Y}$  target. The very slow rise of the  $^{89}\text{Y}$  yield in the region from about 3.6 to 4.2 MeV is consistent with the ground-state transition,  $\Delta I=4$ , and the sharp threshold at  $4255 \pm 6$  keV is attributed to a transition with  $\Delta I=0$  to the 0.588-MeV excited state<sup>14</sup> in  $^{89}\text{Zr}$ .

No threshold is apparent in the thick target  $^{93}\text{Nb}(p, n)$  yield in Fig. 8. In this case it is helpful to use the theory in order to remove the Coulomb barrier effects so that the yield may be plotted on a linear scale. Thus, Fig. 9 compares the ratio of the observed cross section to the predicted compound-nucleus cross section, and shows

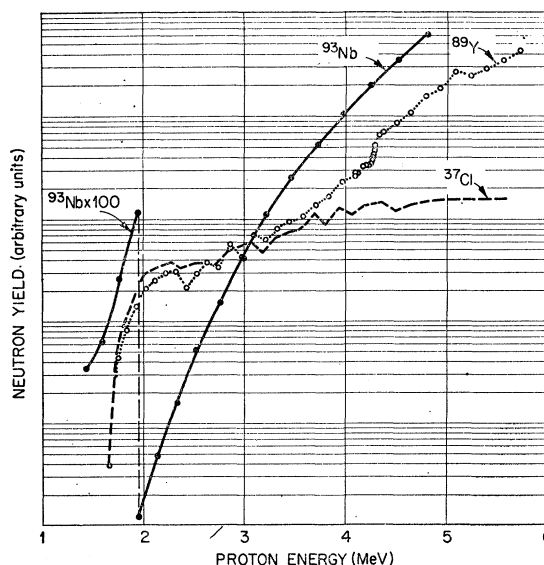


FIG. 8. Yield in arbitrary units from experiment C for targets of  $^{37}\text{Cl}$ ,  $^{89}\text{Y}$ , and  $^{93}\text{Nb}$ . The  $^{37}\text{Cl}$  yield is shown, normalized to the lower energy  $^{89}\text{Y}$  target yield, in order to demonstrate that  $^{37}\text{Cl}$  was a contaminant in the  $^{89}\text{Y}$  target. The step in the  $^{89}\text{Y}$  yield at  $4255 \pm 6$  keV is attributed to a threshold to the 588-keV state in  $^{89}\text{Zr}$ . The semilog plot of the  $^{93}\text{Nb}$  thick target yield obscures an excited-state threshold which causes about a 25% change in slope near 2700 keV. An appropriate linear plot of the cross section (see Fig. 9) shows the threshold.

TABLE III. Weighted averages for all thresholds and  $Q$  values of this report. Comparisons are made to other results from threshold measurements or from neutron energy measurements by time of flight, nuclear emulsions, or resonance scattering. The  ${}^7\text{Li}(p,n)$  standard used by others is listed for several cases.

Reaction	Present results (keV)		$-Q$ (keV)	Other work Method	${}^7\text{Li}(p,n)$ standard
	Threshold	$-Q$			
${}^{37}\text{Cl}(p,n){}^{37}\text{A}$	1640.5±2.5	1596.9±2.5	1598 ±4 <sup>a</sup>	threshold	1882
			1599 ±2 <sup>b</sup>	threshold	1882.2
${}^{41}\text{K}(p,n){}^{41}\text{Ca}$	1239.5±1.5	1209.7±1.5	1597 ±1 <sup>c</sup>	resonance scattering	
			1220 ±20 <sup>a</sup>	threshold	1882
			1100 ±50 <sup>d</sup>	time of flight	
${}^{48}\text{Ca}(p,n){}^{48}\text{Sc}$	<650	<640	660 ±30 <sup>d</sup>	time of flight	
${}^{49}\text{Ti}(p,n){}^{49}\text{V}$	1412.1±1.0	1383.6±1.0	1420 ±30 <sup>d</sup>	time of flight	
			1383 ±9 <sup>e</sup>	resonance scattering	1880.7
${}^{51}\text{V}(p,n){}^{51}\text{Cr}$	1564.1±1.8	1533.7±1.8	1532 ±6 <sup>a</sup>	threshold	1882
			1535.2±1.5 <sup>f</sup>	threshold	1881.4
			1534 ±2 <sup>g</sup>	threshold	1881.1
			1380 ±8 <sup>h</sup>	threshold	1882.2
${}^{53}\text{Cr}(p,n){}^{53}\text{Mn}$	1406.7±1.6	1380.4±1.6	1390 ±30 <sup>d</sup>	time of flight	
			1001 ±10 <sup>i</sup>	threshold	1882.2
			1006 ±10 <sup>j</sup>	resonance scattering	
${}^{55}\text{Mn}(p,n){}^{55}\text{Fe}$	1033.0±0.8	1014.4±0.8	1030 ±30 <sup>d</sup>	time of flight	
			1016 ±2 <sup>g</sup>	threshold	1881.1
			1011 ±5 <sup>k</sup>	resonance scattering	
			1670 ±30 <sup>d</sup>	time of flight	
${}^{57}\text{Fe}(p,n){}^{57}\text{Co}$	1648 ±2	1619 ±2	1670 ±30 <sup>d</sup>	threshold	1882.2
${}^{59}\text{Co}(p,n){}^{59}\text{Ni}$	1887.1±1.6	1855.3±1.6	1857 ±3 <sup>i</sup>	threshold	1882.2
			1863 ±5 <sup>l</sup>	threshold	1882.5
			1855 ±4 <sup>m</sup>	threshold	1881.1
${}^{61}\text{Ni}(p,n){}^{61}\text{Cu}$	3074 ±4	3024 ±4			
${}^{65}\text{Cu}(p,n){}^{65}\text{Zn}$	2169.0±1.7	2135.8±1.7	2137 ±5 <sup>n</sup>	threshold	1881.4
			2136 ±4 <sup>o</sup>	threshold	1881.1
			2131 ±5 <sup>p</sup>	resonance scattering	1881.1
			2132.2±1.5 <sup>q</sup>	threshold	1881.1
			2150 ±50 <sup>d</sup>	time of flight	
			2145 ±10 <sup>o</sup>	resonance scattering	1880.7
			2135.3±1.8 <sup>r</sup>	threshold	1880.7
			1778 ±5 <sup>l</sup>	threshold	1882.5
${}^{67}\text{Zn}(p,n){}^{67}\text{Ga}$	1810.2±1.4	1783.3±1.4	3694 ±6 <sup>o</sup>	threshold	1881.1
			3707 ±5 <sup>l</sup>	threshold	1882.5
${}^{68}\text{Zn}(p,n){}^{68}\text{Ga}$	3762 ±5	3707 ±5	3707 ±5 <sup>l</sup>	threshold	1880.7
${}^{69}\text{Ga}(p,n){}^{69}\text{Ge}$	3050 ±4	3006 ±4	3008.8±3.2 <sup>r</sup>	threshold	1880.7
${}^{70}\text{Zn}(p,n){}^{70}\text{Ga}$	1460 ±3	1439 ±3	1436 ±2 <sup>g</sup>	threshold	1881.1
${}^{71}\text{Ga}(p,n){}^{71}\text{Ge}$	1033 ±2	1018 ±2			
${}^{73}\text{Ge}(p,n){}^{73}\text{As}^x$	1205 ±15	1189 ±15			
${}^{74}\text{Ge}(p,n){}^{74}\text{Ge}$	3394 ±5	3348 ±5	3343.5±5.6 <sup>r</sup>	threshold	1880.7
${}^{75}\text{As}(p,n){}^{75}\text{Se}$	1669.5±1.1	1647.3±1.1	1680 ±30 <sup>d</sup>	time of flight	
			1647 ±2 <sup>g</sup>	threshold	1881.1
${}^{80}\text{Se}(p,n){}^{80}\text{Br}$	2686 ±3	2653 ±3	2655.2±2.8 <sup>r</sup>	threshold	1880.7
${}^{82}\text{Se}(p,n){}^{82}\text{Br}$	<930	<920			
${}^{89}\text{Y}(p,n){}^{89}\text{Zr}^x$	4255 ±6	4207 ±6	4199.8±4.1 <sup>r</sup>	threshold	1880.7
			4200 ±20 <sup>g</sup>	threshold	
${}^{93}\text{Nb}(p,n){}^{93}\text{Mo}$	<1300	<1290	1270 ±40 <sup>t</sup>	nuclear emulsion	
${}^{93}\text{Nb}(p,n){}^{93}\text{Mo}^x$	2750 ±100	2720 ±100	2730 ±40 <sup>t</sup>	nuclear emulsion	
${}^{106}\text{Pd}(p,n){}^{106}\text{Ag}$	3790 ±13	3754 ±13			
${}^{108}\text{Pd}(p,n){}^{108}\text{Ag}$	2700 ±100	2670 ±100			
${}^{112}\text{Cd}(p,n){}^{112}\text{In}$	3430 ±20	3400 ±20			

<sup>a</sup> H. T. Richards, R. V. Smith, and C. P. Browne, Phys. Rev. 80, 524 (1950).

<sup>b</sup> Schoenfeld *et al.*, Ref. 6.

<sup>c</sup> Parks *et al.*, Ref. 11.

<sup>d</sup> Elwyn *et al.*, Ref. 20.

<sup>e</sup> G. J. McCallum, A. T. G. Ferguson, and G. S. Mani, Nucl. Phys. 17, 116 (1960).

<sup>f</sup> Gibbons *et al.*, Ref. 3.

<sup>g</sup> Gossett and Butler, Ref. 23.

<sup>h</sup> J. A. Lovington, J. J. G. McCue, and W. M. Preston, Phys. Rev. 85, 585 (1952).

<sup>i</sup> J. J. G. McCue and W. M. Preston, Phys. Rev. 84, 384 and 1150 (1951).

<sup>j</sup> E. H. Stelson and W. M. Preston, Phys. Rev. 83, 469 (1951).

<sup>k</sup> L. L. Lee, Jr., and F. P. Mooring, Phys. Rev. 115, 969 (1959).

<sup>l</sup> R. A. Chapman and J. C. Slattery, Phys. Rev. 105, 633 (1957).

<sup>m</sup> J. W. Butler, K. L. Dunning, and R. O. Bondelid, Phys. Rev. 106, 1224 (1957).

<sup>n</sup> Kington *et al.*, Ref. 9.

<sup>o</sup> Brugger *et al.*, Ref. 7.

<sup>p</sup> J. B. Marion and R. A. Chapman, Phys. Rev. 101, 283 (1956).

<sup>q</sup> Marion and Kavanagh, Ref. 8.

<sup>r</sup> Okano and Nishimura, Ref. 10.

<sup>s</sup> J. D. Fox, C. F. Moore, J. A. Becker, and C. E. Watson, Bull. Am. Phys. Soc. 8, 375 (1963).

<sup>t</sup> Patterson, Ref. 24.

<sup>x</sup> The superscript x indicates a threshold to an excited state.

a threshold at  $2750 \pm 100$  keV. This is consistent with the  $-2750$ -keV  $Q$  value expected for the 1.48-MeV excited state<sup>14</sup> in  ${}^{93}\text{Mo}$ . The ground-state transition is

inhibited by a rather large spin charge,  $\Delta I=2$ , so that the excited-state threshold,  $\Delta I=0$ , is observable. The change in yield at the excited state is consistent with

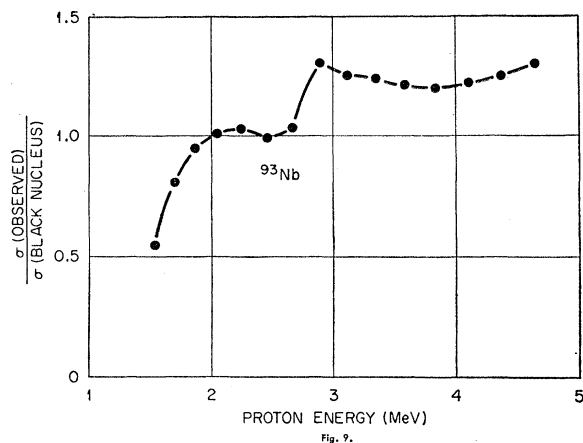


FIG. 9. Ratios of the observed  $^{93}\text{Nb}(p,n)^{93}\text{Mo}$  cross sections to those predicted for compound nucleus formation with a black square-well potential. This linear plot of the cross section shows a threshold at  $2750 \pm 100$  keV which was not apparent in the semilog plot of the yield in Fig. 8. The yield below the threshold is attributed to the ground-state transition ( $\frac{3}{2}^+$  to  $\frac{5}{2}^+$ ) and the threshold is assigned a transition to the  $\frac{3}{2}^+$  1.48-MeV state of  $^{93}\text{Mo}$ . This interpretation is consistent with predictions of the Hauser-Feshbach theory. The fact that the threshold is observable shows that lower excited levels of  $^{93}\text{Mo}$  have  $J \leq \frac{5}{2}$ .

the Hauser-Feshbach theory, and the fact that a threshold is observable indicates that the 0.91 and 1.35-MeV levels<sup>14</sup> in  $^{93}\text{Mo}$  have  $J \leq \frac{5}{2}$ .

### III. SUMMARY

All together, in the course of experiments A, B, and C, thresholds were found for 25 reactions, and threshold limits were found for 2 reactions. Table III gives the statistically weighted averages for all three experiments and the corresponding  $Q$  values. Actually, the quoted errors from the statistical combinations are not quite right because the uncertainties in the absolute standards are frequently common to more than one measurement; however, since the errors in the standards are relatively small, the procedure is nearly correct. As stated in the introduction, these values supersede those of Trail and Johnson<sup>12</sup> and Johnson and Galonsky.<sup>13</sup>

Table III also gives  $Q$  values which others have found by threshold techniques or by measurements of neutron

energy by time of flight, by nuclear emulsion, or by neutron scattering from a resonance at known energy. The  $^7\text{Li}(p,n)^7\text{Be}$  standard used in each experiment is also listed because it has changed slowly over the last ten years. (Additional standards used in some of the experiments are not listed.) If a published threshold has a small uncertainty, say  $\leq 3$  keV, it should be adjusted in accordance with the new standards before comparison is made with the present work. The adjustment has not been done in the table.

The agreement among the experiments is quite good. In general, each measurement in the literature agrees with the present one to within twice the larger standard error; only  $^{68}\text{Zn}(p,n)^{68}\text{Ga}$  threshold of Brugger *et al.*<sup>7</sup> and the adjusted  $^{65}\text{Cu}(p,n)^{65}\text{Zn}$  threshold of Marion and Kavanagh<sup>8</sup> lie outside these limits. (The positron end point<sup>14</sup> from  $^{65}\text{Zn}$  also disagrees with the present result.) Considerable information<sup>14</sup> related to the various  $Q$  values, particularly positron spectra end points, generally agree with the present work; however, a large discrepancy does exist in the case of  $^{57}\text{Fe}(p,n)^{57}\text{Co}$ . Measurements by Jung and Pool<sup>26</sup> on the bremsstrahlung from the decay of  $^{57}\text{Co}$  indicate a  $Q$  value of  $-1350 \pm 30$  keV in disagreement with the present value of  $-1619 \pm 2$  keV. Other data<sup>14</sup> favor the present result.

In the present paper, the yields near threshold have been compared with the approximate predictions of the Hauser-Feshbach<sup>4</sup> statistical theory of the compound nucleus. The theory was found to be a rather good approximation and was helpful in assigning thresholds. In particular, it guided us to the assignment of threshold limits, rather than thresholds, for targets of  $^{48}\text{Ca}$ ,  $^{82}\text{Se}$ , and  $^{93}\text{Nb}$ . Comparison of the yield and theory for  $^{48}\text{Ca}(p,n)$  indicates that the observed<sup>20</sup> ( $-660 \pm 30$ )-keV  $Q$  value is not the ground-state  $Q$ . For similar reasons, the threshold at  $1205 \pm 15$  keV for  $^{78}\text{Ge}(p,n)$  is assigned to the excited state,  $\frac{9}{2}^-$  to  $\frac{5}{2}^-$ , transition. The fact that the 1.48-MeV excited-state threshold for  $^{93}\text{Nb}(p,n)$  was observed indicates that lower states have  $J \leq \frac{5}{2}$ .

<sup>26</sup> R. G. Jung and M. L. Pool, *Bull. Am. Phys. Soc.* **1**, 172 (1956).